ANALYSIS OF ZEOTROPIC MIXTURE IN A GEOTHERMAL ORGANIC RANKINE CYCLE POWER PLANT WITH AN AIR-COOLED CONDENSER

H. C. Jung[1] and Susan Krumdieck[2]

[1,2]*Department of Mechanical Engineering, University of Canterbury, Private Bag 4800, Christchurch 8041, New Zealand*

[1]hyung-chul.jung@canterbury.ac.nz

[2]susan.krumdieck@canterbury.ac.nz

Keywords: *Working fluid, Zeotropic mixture, Air-cooled Condenser, Geothermal, Organic Rankine cycle.*

ABSTRACT

The purpose of this research is to investigate a zeotropic working fluid mixture in terms of its performance in an organic Rankine cycle (ORC) and the heat transfer characteristics in an air-cooled condenser (ACC). The motivation of this study is that it is well known that the use of a mixture improves the efficiency of an ORC system. However, the behaviour of the mixture in the condensers is not well understood. A standard ORC unit utilising hot spring water to generate electricity is considered for the analysis. A mixture of two fluids, isobutane and pentane, is used as the working fluid. Numerical models of the ORC power plant and ACC are developed and simulations are conducted with the pure fluids and their mixtures with four different compositions. The optimum operating conditions of the system are estimated for each fluid, and they are then applied to a condenser, designed to use pentane, to calculate and compare the heat transfer parameters. The mixtures display a significant increase in the system performance compared to the pure fluids. A highest exergetic efficiency of 24.2% is achieved for the system using a mixture of 80% isobutane/20% pentane. However, with the exception of the mixtures having the isobutane composition between approximately 35% and 60%, all of the mixtures require an additional surface area of the condenser compared to that for pure pentane due to their relatively low heat transfer characteristics. Therefore, the design of the ORC system and ACC involves a compromise between the system efficiency and condenser size when mixtures are employed as the working fluid.

1. INTRODUCTION

The rising scarcity of non-renewable energy resources and the environmental issues with their use means that demand for renewable energy is increasing. Geothermal energy is one of the clean, sustainable energy resources and the amount of geothermal energy is virtually endless in the earth. The temperatures of geothermal fluids range from 50 to 350 °C and most of resources consist of the low to moderate temperature (below 150°C) liquids. It is possible to extract and convert the abundant brine into electrical power via the organic Rankine cycle (ORC), and the installation of ORC power plants has been rapidly growing over the past two decades all around the world.

To promote the continuing growth of the use of ORC plants in the regions where a supply of cooling water is not available, it is necessary to employ air-cooled condensers (ACC) to provide a means of condensing the working fluid. The additional advantage associated with the use of ACC depends on the fact that the dry condensing method is not subject to government regulations and environmental concerns relevant to treatment and disposal of water.

The working fluid plays a vital role in the energy conversion efficiency of ORC machine. Numerous studies have been focused on the proper selection of pure fluids, including refrigerants such as R-134°, R-123 and R-245fa and volatile hydrocarbons such as butane and pentane (Saleh et. al., 2007, Wang et. al., 2011). General selection criteria for a potential fluid were proposed by Chen et. al. (2010).

The suggestion of using a working fluid mixture in vapour compression systems was first made in 1888 by Pictet (Radermacher 1989). The benefits of using organic fluid mixtures as the working fluid in ORC systems were investigated by Angelino and Paliano (1998). By using a mathematical model they demonstrated that optimal selection of fluid composition can improve the ORC performance, based on the use of mixtures of siloxanes and hydrocarbons. Recently, more research has been conducted to evaluate the performance of ORC systems with mixtures as the working fluid (Borsukiewicz-Gozdur and Nowak, 2005, Wang et. al., 2010, Heberle et. al., 2012). Despite these efforts, the effects of mixture on the ACC performance still remain to be studied and compared with the performance of pure fluids to obtain an optimised design of the system and components.

In the present study, a standard ORC unit utilising hot spring water (this heat source is available from Waikite Valley in Rotorua) to generate electricity is used as a case study to investigate a zeotropic working fluid mixture in terms of its effect on the ORC system performance and heat transfer characteristics in the ACC. A mixture of two fluids, isobutane and pentane, is used as the working fluid. The performance parameters to be measured include the net power output and Second Law efficiency for the ORC unit and the heat duty, convective and condensation heat transfer coefficients, surface area, and log mean temperature difference for the ACC. Computational models of the ORC system and ACC component are developed to estimate the performance.

2. NUMERICAL METHOD

The thermodynamic analysis of the power cycle for a standard ORC system is first presented. The Second Law efficiency is then described for the exergy analysis of the ORC power plant. Lastly, correlations to determine the convective and condensation heat transfer coefficients for the ACC are introduced.

2.1 ORC model

A schematic flow diagram of the standard ORC power plant is shown in Figure 1. The thermodynamic processes undergone by a working fluid mixture are illustrated on a temperature-entropy diagram in Figure 2. In the evaporator, a geothermal fluid increases the temperature of the working fluid in a liquid form until it reaches a slightly superheated state. The vapour expands through the turbine, generating electricity in the generator. The vapour from the turbine

passes through the ACC that turns it back into liquid. The working fluid is conveyed to the pump where it is fed into the evaporator to complete the cycle. The numbers designate the state points of the working fluid.

The system is analysed on the assumption that it is at a steady state and the geothermal liquid behaves as pure water. The state at the exit of the turbine (state 2) is specified by defining the isentropic turbine efficiency as:

$$\eta_t = \frac{h_1 - h_2}{h_1 - h_{2s}} \tag{1}$$

(see the nomenclature list for definition of the symbols in this and other equations). In order to find the process conditions at the pump outlet (state 6), its isentropic efficiency is given by:

$$\eta_p = \frac{h_{6s} - h_5}{h_6 - h_5} \tag{2}$$

The property data are evaluated on the assumption of constant pressure across the heat exchangers and piping system because pressure drops are less significant sources of irreversibility in a well-designed system compared with the irreversibility occurring in the turbine and pump components. It is also assumed that heat losses from the system components to the surroundings are negligible.

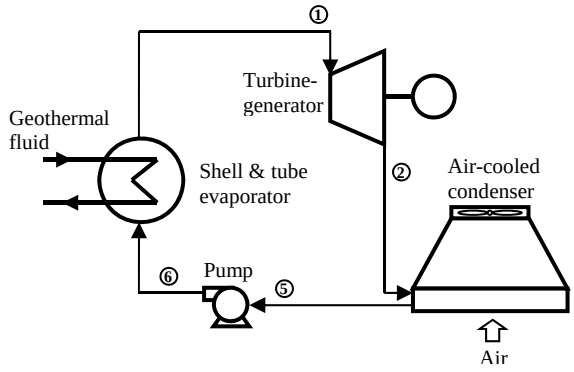

Figure 1: Schematic of a standard ORC power plant.

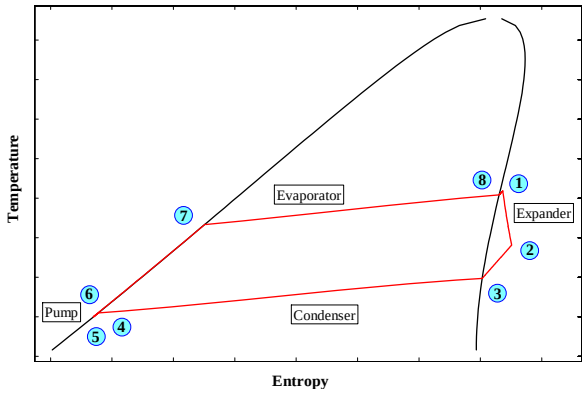

Figure 2: Temperature-entropy diagram for a standard ORC power plant using a working fluid mixture.

The flow rate of working fluid is computed by equating the thermal energy supplied from the geothermal fluid with the energy acquired by the working fluid. The evaporation and condensation temperatures of the working fluid are determined by the pinch-point analysis. The cycle and net powers and the plant efficiency are respectively expressed by:

$$W_{cycle} = \eta_m \eta_g \dot{m}_{wf} (h_1 - h_2) - W_p \tag{3}$$

$$W_{net} = W_{cycle} - W_f \tag{4}$$

$$\eta_{plant,I} = \frac{W_{net}}{Q_{in}} \tag{5}$$

The power consumption of the fan in the ACC is determined by assuming it is 20% of the cycle power. Since the emphasis of the present study is on the analysis of mixtures, the power needed for the geothermal fluid supply pump is not considered in the net work of the plant.

2.2 Exergy efficiency

The exergy efficiency based on the Second Law of thermodynamics is introduced on the basis of the work done by Dipippo (2005). In this case of geothermal power plant, exergy means the maximum work that can theoretically be achieved from the geothermal source at the reservoir conditions relative to its surroundings. The specific exergy can be written as:

$$e = h_{res} - h_0 - T_0(s_{res} - s_0) \tag{6}$$

where h_{res} and s_{res} are the enthalpy and entropy of the geothermal fluid at the reservoir state, and T_0, h_0 and s_0 are the properties evaluated at the dead state (i.e., when the fluid is in equilibrium with the surroundings). When the fluid is a liquid at the dead state, it is appropriate to take the enthalpy and entropy values for a saturated liquid at the wet-bulb temperature.

The maximum work output that can be obtained from the geothermal water is therefore expressed as:

$$W_{\max} = \dot{m}_{wf} e \tag{7}$$

The Second Law efficiency of the plant is defined as:

$$\eta_{plant,II} = \frac{W_{net}}{W_{\max}} \tag{8}$$

2.3 ACC model

The ACC is taken into account with circular finned-tubes staggered horizontally. In the ACC, while the working fluid flows inside the tubes, heat is transferred from the working fluid to cooling air in the following three consecutive modes: vapour to air in Process 2-3, vapour/liquid mixture to air in Process 3-4, and liquid to air in Process 4-5. The actual heat rejection in each process is calculated by:

$$Q = U_o A F \Delta T_{LM} \tag{9}$$

Here the overall convective heat transfer coefficient is based on the air-side surface area and is given by:

$$U_o = \frac{1}{\frac{1}{h_{wf}}\left(\frac{A_{air}}{A_{wf}}\right) + R''_{wf}\left(\frac{A_{air}}{A_{wf}}\right) + R_w A_{air} + R''_{air} + \frac{1}{\eta_o h_{air}}} \tag{10}$$

2.3.1 Correlation for tube-side convective heat transfer coefficient

With the assumption that the working fluid is under the condition of a fully developed single-phase turbulent flow in Processes 2-3 or 4-5, the friction factor is computed by the Zigrang and Sylvester correlation (Ghanbari et. al., 2011).

$$\frac{1}{\sqrt{f}} = -2\log\left(\frac{e/D}{3.7} - \frac{5.02}{\mathrm{Re}}\log\left(\frac{e/D}{3.7} - \frac{5.02}{\mathrm{Re}}\log\left(\frac{e/D}{3.7} + \frac{13}{\mathrm{Re}}\right)\right)\right) \quad (11)$$

The Gnielinski correation is used to calculate the Nusselt number.

$$Nu = \frac{(f/8)(\mathrm{Re}-1000)\,\mathrm{Pr}}{1+12.7(\mathrm{Pr}^{2/3}-1)\sqrt{(f/8)}} \quad (12)$$

2.3.2 Correlation for tube-side condensation heat transfer coefficient

The working fluid-side condensation heat transfer coefficient for a fully developed fluid stream is estimated by the Dobson and Chato correlation (Dobson and Chato, 1998) modified by Nellis and Klein (2009). When the mass flux is greater than 500 kg/m^2·s, the coefficient is calculated as:

$$h_{wf,a} = \frac{k_{l,sat}}{D}0.023\,\mathrm{Re}_l^{\,0.8}\,\mathrm{Pr}_{l,sat}^{\,0.4}\left(1+\frac{2.22}{X_{tt}^{\,0.89}}\right) \quad (13)$$

In case the mass flux is less than 500 kg/m^2·s, the modified Froude number is evaluated according to a cut-off value of 1250 for the superficial liquid Reynolds number. Then, if the Froude number is greater than 20, the flow is assumed to be annular and the heat transfer coefficient is determined by Eq.(13). If the Froude number is less than 6, the flow is assumed to be wavy and the heat transfer coefficient is computed as follows:

$$h_{wf,w} = \left(\frac{k_{l,sat}}{D}\right)\left[\left(\frac{0.23}{1+1.11X_{tt}^{\,0.58}}\right)\left(\frac{GD}{\mu_{v,sat}}\right)^{0.12}\left(\frac{\Delta h_v}{C_{l,sat}(T_{sat}-T_s)}\right)^{0.25} Ga^{0.25}\,\mathrm{Pr}_{l,sat}^{\,0.25} + A\cdot Nu_{fc}\right] \quad (14)$$

If the Froude number is between 6 and 20, the heat transfer coefficient for transition flow is defined as:

$$h_{wf,t} = \left(h_{wf,a}^{\,6} + h_{wf,w}^{\,6}\right)^{1/6} \quad (15)$$

2.3.3 Correlation for air-side convective heat transfer coefficient

In order to find the air-side heat transfer coefficient, the Zukauskas correlation for the Nusselt number (Incropera and DeWitt, 2002) is used:

$$Nu = C_2 C\,\mathrm{Re}^m\,\mathrm{Pr}^{0.36}\left(\frac{\mathrm{Pr}}{\mathrm{Pr}_s}\right)^{1/4} \begin{cases} & 1\mathrm{x}10^3 < \mathrm{Re} < \mathrm{x}10^5 \\ for & 0.7 < \mathrm{Pr} < 500 \\ & N_L < 20 \end{cases} \quad (16)$$

where the correction factor C_2 =0.35 $(S_h/S_v)^{1/5}$ and m=0.60 when S_h/S_v <2. In case of $N_L \geq 20$, the correction factor should be eliminated to calculate the Nusselt number.

3. CHOICE OF WORKING FLUIDS

A mixture is called zeotropic if the composition of the vapour and the liquid are never the same during the phase change for a given pressure. Hence, a difference between the liquid and vapour saturation temperatures, called temperature glide, is occurring in the mixture. The gliding temperature increases the match of the temperature profiles between the heat transfer medium and the evaporating or condensing working fluid, leading to the reduction in the irreversibility during the heat transfer process. Therefore, when zeotropic mixtures are used as working fluid in ORC systems, a performance improvement of the system is expected in comparison to that for a pure fluid.

Zeotropic working fluid mixtures are made by mixing the fluids with the large boiling point difference and similar chemical properties. In this study, two pure fluids, pentane and isobutene, are chosen to produce zeotropic mixtures. Figure 3 shows the bubble and dew point lines and the temperature glide for the pentane/isobutane mixture over the entire composition range. It is noted that a maximum temperature glide of 12°C occurs with a 40-60 mixture of pentane and isobutane. The processes of preheating, evaporation and superheating of the equimolar mixture corresponding to the processes on the previous power cycle (refer to Figure 2) are given in Figure 3 as an example.

4. RESULTS AND DISCUSSION

The hot spring water data and the assumptions for the plant components adopted for the simulation of the ORC system and ACC are listed in Table 1. The two pure fluids, isobutane and pentane, and their four different mixtures having the mole fractions of 20%, 40%, 60% and 80% isobutane were considered in this study. Simulations were performed using the software Engineering Equation Solver (EES) and the thermodynamic properties of fluids were evaluated by REFPROP 9.0 (2010).

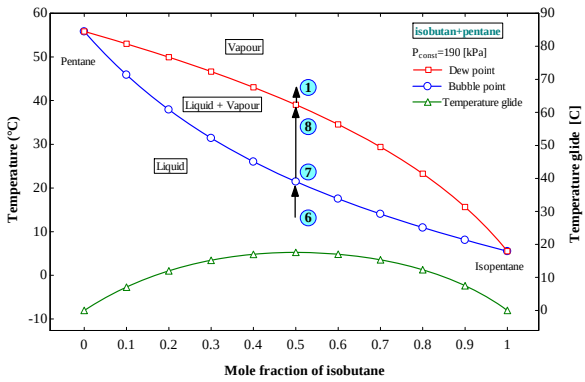

Figure 3: Temperatures of saturated liquid and vapour and temperature glide for a mixture of isobutane/pentane as a function of mole fraction of isobutane.

Table 1: Heat source data and assumptions.

Description	Value
Temperature of hot spring water	99°C
Mass flow rate of hot spring water	3000 t/d
Temperature of cooing air (in/out)	18/30°C
Pinch point temp. difference for evaporator	5°C
Pinch point temperature difference for ACC	10°C
Isentropic efficiency of turbine	0.8
Isentropic efficiency of pump	0.7
Mechanical loss of turbine	1% of shaft power
Generator loss	2% of shaft power

4.1 Effect on the ORC system performance

In order to find the optimum hot spring water temperature at the evaporator outlet and investigate the effects of the mixtures on the ORC performance, simulations were performed and the results are presented in Figures 4 and 5. Figure 4 shows the variation of the net power output obtained from the ORC unit with the hot water temperature at the exit of the evaporator for the pure fluids and mixtures. It is obvious that the mixtures yield higher electrical power output than the pure fluids. Among the mixtures under investigation, the highest power is attained with a mixture of 20% pentane/80% isobutane. It is also indicated that the maximum power is gained with the water outlet temperatures of 60°C and 65°C for the mixtures and pure fluids, respectively. The difference in the optimum temperature is caused by the fact that the pinch point is located at state point 7 (Figure 2) and the preheating and boiling curves of the mixtures have a better match to the hot spring water cooling curve in comparison to the pure fluids. The mixture behaviour leads to the increase in the specific work output of the turbine. This is the reason for the relatively high power outputs obtained with the mixtures.

Figure 5 depicts the variation of the exergy and thermal efficiencies of the plant with the hot water outlet temperature from the evaporator for the pure fluids and mixtures. The results show that the maximum exergy efficiencies are obtained at 60°C and 65°C for mixtures and pure fluids, respectively, whereas the thermal efficiencies keep rising with increasing water temperature.

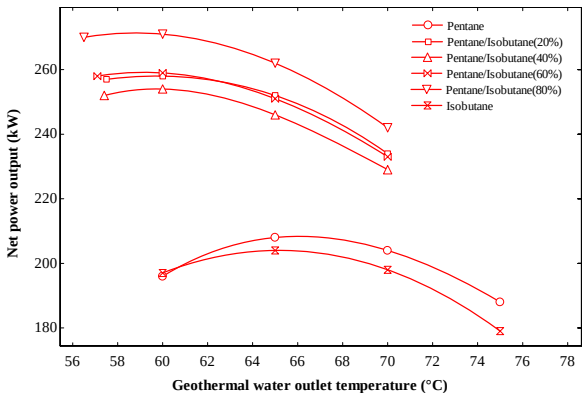

Figure 4: Net power output as a function of geothermal water outlet temperature.

The reason for this is that as the water exit temperature increases the thermal power input to the evaporator decreases while the exergy of the heat source remains constant. Hence, as can be seen in Eqs. (5) and (8), the exergy efficiency follows the trend of the net power and the thermal efficiency increases. Therefore, it is effective to measure the exergy efficiency as an indicator of performance in the ORC system design. Figure 6 shows the variation of the maximum power output and exergy efficiency with the mole fraction of isobutane. It is evident that the exergy efficiency curve has a similar pattern to that of the power output. The slight deviation is caused by the power consumption of the ACC fan which was estimated to be 20% of the cycle power.

Figure 7 presents the influence of the mixture composition on the mass flow rate and enthalpy change of the fluid in the evaporator. The flow rate increases with rising isobutane composition. This is because the enthalpy change in the mixtures reduces while the heat duty transferred to the heat exchanger remains constant as the isobutane composition increases. It is observed that the largest enthalpy change occurs at the mole fraction of around 20% where the second greatest net power output and exergy efficiency are gained (Figure 6). Therefore, there should be a compromise between the amount of fluid and net power output in the system design.

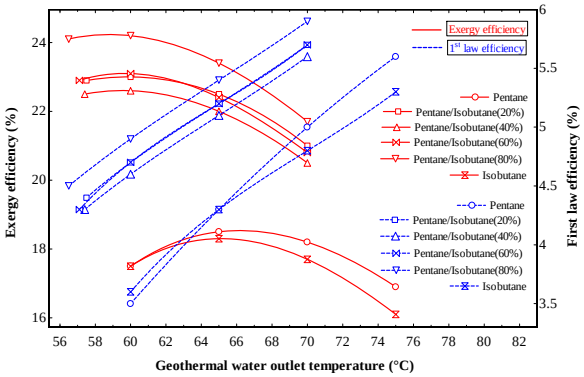

Figure 5: Exergy and plant efficiencies as a function of geothermal water outlet temperature.

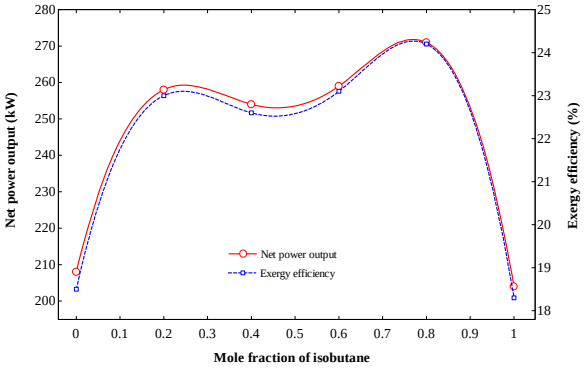

Figure 6: Net power output and exergy efficiency as a function of mole fraction of isobutane.

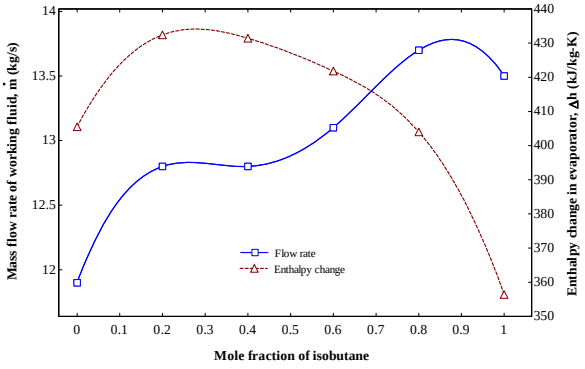

Figure 7: Mass flow rate of working fluid as a function of mole fraction of isobutane.

4.2 Heat transfer characteristics in the ACC

A reference ACC design was first performed on the basis of the optimum operating conditions of pentane, and then the condenser geometry determined was used for the analysis of mixture heat transfer characteristics. The optimum conditions of the mixtures found in the previous section were applied to the reference condenser as process parameters. A tube surface roughness of 1.5 μm, a typical value for drawn tubing, was input for the calculation of the friction factor. Other input design parameters adopted for the

calculation of heat transfer coefficients are described in Table 2. A convergence problem was seen during the calculation of the specific heat at constant pressure and bulk temperature in Process 2-3, thus the average of the values obtained at each state 2 and 3 was used in the coefficient estimate. The geometric specifications of the reference ACC designed are presented in Table 3.

Table 2: ACC geometric specifications designed using pure pentane as working fluid.

Description	Value
Tube material	AISI 304
Fouling factor, refriger' liquid	0.000176 m^2-K/W
Fouling factor, refriger'vapour	0.000352 m^2-K/W
Fouling factor, compressed air	0.000175 m^2-K/W

Table 3: ACC geometric specifications designed using pure pentane as working fluid.

Description	Value
Fin thickness	0.46 mm
Fin diameter	66.65 mm
Fin pitch	2.3 mm
Tube outside diameter	34.9 mm
Tube thickness	2 mm
Vertical tube separation	75 mm
Horizontal tube separation	72 mm
Number of tube rows (per bundle)	6
Number of tube columns (per bundle)	50
Number of passes (per bundle)	3
Number of passages (per bundle)	100
Tube length (per pass)	3 m
Number of bundles	6
Total heat transfer surface area	12364 m^2
σ (free flow area/frontal area)	0.4122
α (surface area/volume)	424 m^2/m^3
Fin area/surface area	0.9617
Outer surface area/inner surface area	24

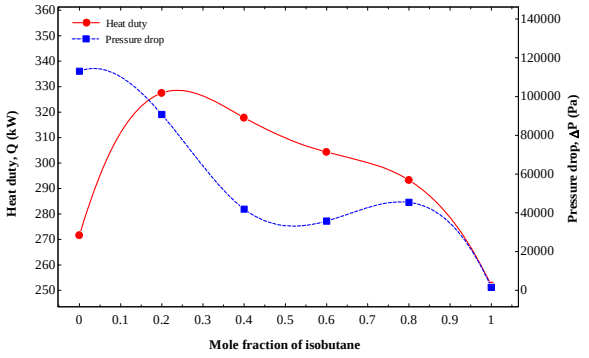

Figure 8: Heat duty (required and actual) and pressure drop for the superheated vapour cooling process as a function of mole fraction of isobutane.

4.2.1 Superheated vapour cooling process

Figure 8 shows the variation of the heat duty and pressure drop in the ACC for the cooling process (Process 2-3) of the superheated vapour from the turbine exit with the mole fraction of isobutane. Since this process is involved in the front section of the condenser, there is a sufficient surface area available. Hence, the actual heat duty is equal to the heat duty required regardless of the heat transfer coefficient and log mean temperature difference. It is noted that the largest duty is required for a mixture of 20% isobutane/80% pentane. This is attributed to the biggest enthalpy drop of the mixture. The pressure drop of mixtures falls between the pressure losses of pure fluids due to their density properties: at state 2, the densities are 3.15, 5.45, and 12.80 kg/m^3 for the pentane, mixture of 40% isobutane/60% pentane, isobutane, respectively.

Figure 9 presents the variation of the tube- and air-side convective heat transfer coefficients and the overall coefficient as a function of mole fraction of isobutane. As expected, the tube-side coefficients are higher than those of the air-side. This is because even though the average thermal conductivity of the working fluid is less than that of air, the Reynolds number of tube-side is much larger than that of air-side. For example, in the case of the 80-20 mixture of isobutane and pentane, the conductivities of the mixture and air are 0.018 and 0.162 W/m-K, respectively. However, the Reynolds numbers of the mixture and air are 121832 and 24208, respectively. The overall coefficients ranging from 4.4 to 5.2 W/m^2-K are comparable to the average values of 7.9 and 14.2 W/m^2-K for the air-to-air and air-to-steam, respectively (WWW.engineeringtoolbox.com). The deviation seems to be associated with the fouling factors incorporated in this study. There is about 20% increase in the coefficient with an isobutane composition of 80% compared to pentane.

Figure 10 depicts the variation of the log mean temperature difference (ΔT_{LM}) and surface area of the condenser with the mole fraction of isobutane. ΔT_{LM} is expressed as a function of the entry and exit temperatures of each fluid. In the case of the mixture of 40% isobutane, the inlet and outlet temperatures are 60.1 and 46.8°C for the mixture, respectively, and 29.3 and 30°C for the air, respectively, and the correction factor is 0.997. The greatest difference is gained with the equimolar mixture, which has about 80% of the rise for isobutane. Therefore, the equimolar mixture needs the minimum surface area even though it has a relatively moderate overall heat transfer coefficient.

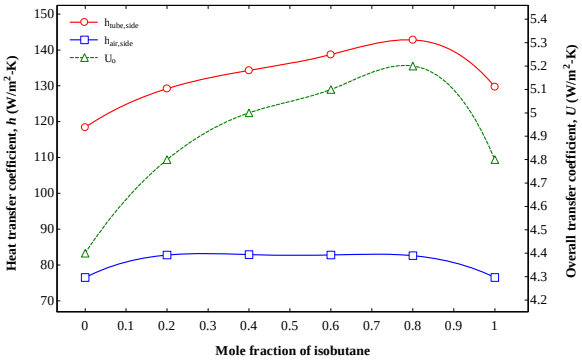

Figure 9: Heat transfer coefficients for superheated vapour cooling as a function of mole fraction of isobutane.

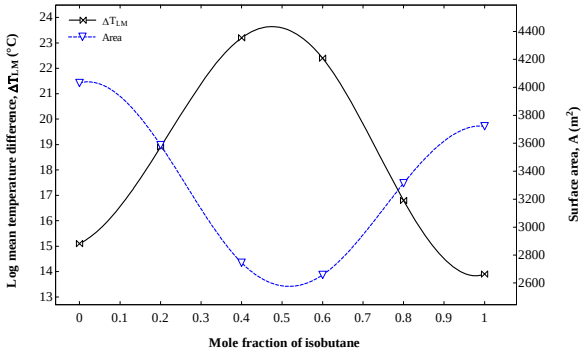

Figure 10: Log mean temperature difference and surface area for superheated vapour cooling as a function of mole fraction of isobutane.

4.2.2 Condensation process

The tube wall temperature plays a significant role in the computation of the condensation heat transfer coefficients (i.e., tube-side coefficients). In order to find the surface temperature and average tube-side heat transfer coefficient, the average coefficient was first predicted with the calculation of 20 local coefficients along the tube with the assumption that the working fluid and tube surface temperatures linearly reduce from the beginning to the end of the condensation process. Initially, a guessed value is used for the surface temperature. After the estimation of the average coefficient, the heat balance is then examined according to the following relationship:

$$h_{t,avg}\left(T_{WF,ave}-T_{surf,avg}\right)=h_{a,gue}\left(T_{surf,avg}-T_{a,avg}\right) \quad (17)$$

where $h_{a,gue}$ is the assumed value for the heat transfer coefficient of the air-side. The calculation of the average tube-side coefficient is repeated by changing the surface temperature and air-side coefficient until the air-side coefficient converges to the value calculated by Eq. (16). Eq. (17) is valid under the assumption that heat flux is constant in the radial direction of the tube. During the calculation of each discrete local coefficient, the local working fluid temperature was regarded as the fluid saturation temperature for the prediction of the modified latent heat of evaporation and the liquid Jakob number.

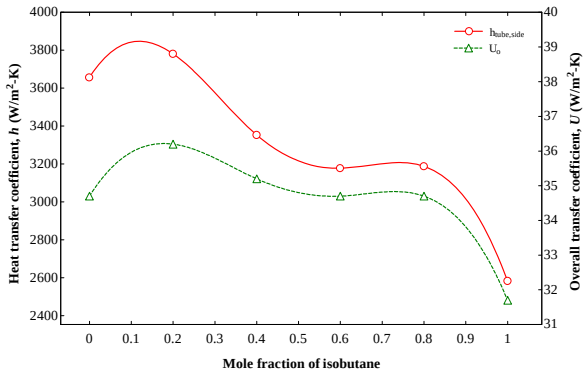

Figure 11: Tube-side and overall heat transfer coefficients for condensation as a function of mole fraction of isobutane.

Figure 11 illustrates the variation of the tube-side condensation and overall heat transfer coefficients with the mole fraction of isobutane. The air-side coefficients ranges between 76.5 and 82.9 W/m^2-K which are the same as those for the vapour cooling and are omitted here for clarity. It is evident that the overall coefficient is dominated by the tube-side coefficient which is relatively greater than that of the air-side. Since the overall coefficient for the organic substance flow condensation was not available from literature, the film coefficient of organic solvents is referenced for comparison which lies in between 850 and 2500 W/m^2-K (www.hcheattransfer.com). The tube-side coefficients between 2600 and 3800 W/m^2-K are reasonable because the coefficient is higher for the flow condensation. In contrast to the overall coefficient for the vapour cooling process, it is noticed that the overall coefficient reduces with increasing isobutane mole composition. The maximum difference of the overall coefficient is approximately 14%.

Figure 12 presents the log mean temperature difference and condenser surface area available as function of mole fraction of isobutane. Since the whole surface area remains constant, the available area shows the opposite trend to that in the vapour cooling process. Of the mixtures, the maximum ΔT_{LM} is observed with the equimolar mixture and the two relatively low values exist with the mixtures of isobutane compositions of about 20% and 80%, respectively. The highest differences of the temperature and area are approximately 25% and 17%, respectively.

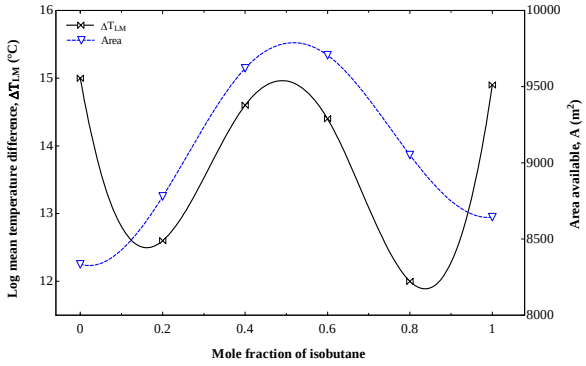

Figure 12: Log mean temperature difference and surface area available for condensation as a function of mole fraction of isobutane.

Figure 13 depicts the variation of the required and actual heat duties with the mole fraction of isobutane. The results show that due to the relatively high ΔT_{LM} and surface area, the condenser capacity is sufficient to meet the condensation requirement for the mixtures with the mole fractions of isobutane between approximately four and six. It is also noticed that the condenser is approximately 20% under-designed at the isobutane fractions of about 10% and 90%. This is because their ΔT_{LM} and surface area available are relatively low even though the mixture of 10% isobutane displays a relatively high overall heat transfer coefficient.

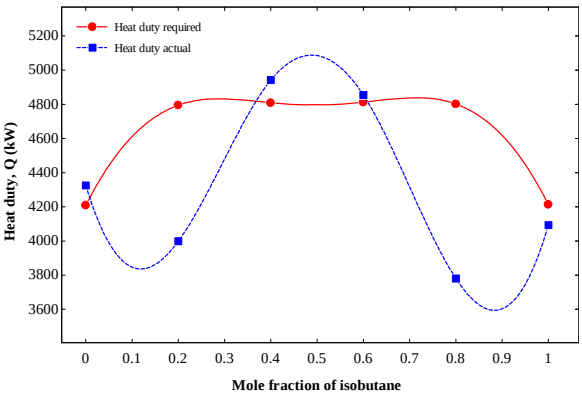

Figure 13: Required and actual heat duties for condensation as a function of mole fraction of isobutane.

5. CONCLUSIONS

A working fluid mixture of isobutane/pentane has a significant impact on the ORC system efficiency compared to that for pure fluids. The mixture generates higher electrical power than the pure fluids over the entire composition range. Even though the highest efficiency is achieved with a mixture of 80% isobutane/20% pentane, this advantage offset bythe smaller actual heat transfer rate than the heat duty required, which means a bigger size of ACC is required compared to that for pure isobutane. In terms of both system efficiency and ACC size, the mixtures with isobutane compositions between 35% and 60% have an advantage compared to pure fluids.

6. FUTURE WORKS

Pressure drops in the condensation process will be evaluated. Optimised ACC design will be done for mixtures to examine the actual sizes, fan powers, and exergy losses and efficiencies. The composition shift for the mixture which may be caused by the differential holdup during the condensation process is not considered in the simulations. Experimental investigation will be carried out to validate the simulation results.

ACKNOWLEDGEMENTS

This work was supported by the New Zealand Heavy Engineering Research Association funded by Ministry for Science & Innovation contract: HERX1001.

REFERENCES

Angelino, G., Paliano, P.C.D.: Multicomponent working fluids for organic Rankine. *Energy*, 23, pp. 449 – 463. (1998).

Borsukiewicz-Gozdur, A., Nowak, W.: Comparative analysis of natural and syntheic refrigerants in application to low temperature Clausius-Rankine cycle. *Energy*. 32, pp. 344 – 352. (2005).

Chen, H. Goswami, D.Y. Stefanakos, E.K.: A review of thermodynamic cycles and working fluids for the conversion of low-grade heat. *Renewable and Sustainable Energy Reviews*, 14, pp. 3059 – 3067. (2010).

DiPippo, R.: Geothermal power plants: principles, applications and case studies. Oxford OX5, UK: Elsevier. (2005).

Dobson, M.K. Chato, J.C.: Condensation in smooth horizontal tubes, *ASME Journal of Heat Transfer*. 120, pp. 193 – 213 (1998).

Ghanbari, A., Farshad, F.F., Rieke, H.H.: Newly developed friction factor correlation for pipe flow and flow assurance. *Journal of Chemical Engineering and Material Science*. 2(6), pp. 83 – 86. (2011).

Heberle, F., Preibinger, M., Bruggemann, D.: Zeotropic mixtures as working fluids in organic Rankine cycles for low-enthalpy geothermal resources. *Renewable Energy*. 37, pp. 364 – 370. (2012).

Incropera, F.P., DeWitt, P.D.: *Fundamentals of heat and mass transfer*. 5th ed. New York: John Wiley & Sons. (2002).

Nellis, G.F., Klein,S.A.: *Heat transfer*. New York: Cambridge University Press. (2009).

Radermacher, R.: Thermodynamic and heat transfer implications of working fluid mixtures in Rankine cycles. *International Journal of Heat and Fluid Flow*, Vol. 10, No. 2. pp. 90 – 102. (1989).

REFPROP, V. 9.0, National Institute of Standards and Technology, Standard Reference Data Program, Gaithersburg. (2010).

Saleh, B., Koglbauer, G., Wendland, M., Fischer, J.: Working fluids for low-temperature organic Rankine cycles. *Energy*, 32, pp. 1210 – 1221. (2007).

Wang, E.H., Zhang, H.G., Fan, B.Y., Ouyang, M.G., Zhao, Y., Mu, Q.H.: Study of working fluid selection of organic Rankine cycle (ORC) for engine waste heat recovery. *Energy*, 36, pp. 3406 – 3418. (2011).

Wang, J.L., Zhao, L., Wang, X.D.: A comparative study of pure and zeotropic mixtures in low-temperature solar Rankine cycle. *Applied Energy*, 87, pp. 3366 – 3373. (2010).

www.engineeringtoolbox.com/overall-heat-transfer-coefficients-d_284.html.

www.hcheattransfer.com/coefficients.html

NOMENCLATURE

A: area (m^2), angle (rad); *D:* diameter (m); ΔT_{LM} : log mean temperature difference (°C); *e*: exergy (kJ/kg), surface roughness (μm); *F*: correction factor; *f*: friction factor; *G*: mass flux (kg/s· m^2); *h*: enthalpy (J/kg), heat transfer coefficient (W/m^2-K); *k*: thermal conductivity (W/m-K); $\dot{m}$: mass flow rate (kg/s); *Nu*: Nusselt number; N_L: number of tube in longitudinal direction; *Pr*: Prandtl number; *Q*: heat transfer rate (W); *Re*: Reynolds number; R_w: wall resistance (°C/W); R'': fouling factor (m^2-K/W); S_h: horizontal separation (m); S_v: vertical separation (m);*T*: temperature (°C); X_{tt} : Lockhart Martinelli parameter; U_o: overall heat transfer coefficient (W/m^2-K); *W*: power (W)

Greek symbols

η: efficiency; η_o: overall efficiency of finned surface; μ: dynamic viscosity (kg/m·s)

Subscripts

1, 2 ...: state points; *a:* air; *f*: fan; *g:* generator; *l*: liquid; *m*: motor; *p*: pump; *t*: turbine, tube side; *v*: vapour; *w*: water; *wf*: working fluid